Early Detection of Diabetes Retinopathy and Disease Progression Prediction Based on Retinal Vascular Network Analysis

Jie Lian

Master of Science

Data Science

School of Informatics

University of Edinburgh

2020

Abstract

Analyzing changes in the retinal vascular network of patients with diabetes retinopathy (DR) can help physicians diagnose the disease at an early stage and allow patients receive better medical therapy. In this project, we employ graph theory and Bayesian logistic regression algorithms to detect changes on patients with DR. We suggest three sets of precise metrics that can represent major features on the DR patient's retinal vascular network. We also use efficient techniques of machine learning to pick significant characteristics in the classification of healthy people and DR (with accuracy of 70%), as well as the duration of medical therapy (with accuracy of 87.33%), which gives some practical advice for doctors and medical institutions to diagnose DR at early stages and explore the changes during clinical treatment. In the last step, a "forecast for disease progression" model is given to assist the hospital to provide better medical suggestions for diabetes patients.

Acknowledgements

I would like to thank my supervisors: Dr. Rik Sarkar, Dr. Miguel Bernabeu, and Ph.D. candidate Ylenia Giarratano. From beginning to finish, they give advice and feedback for the studies, suggest improvements and correct mistakes for the this thesis.

MSc student Alisa Pavel is working with classification assignment on a comparable project on vascular networks. We share some metrics codes and in the relevant parts I cite these instances. I would love to thank her, for her helpful cooperation throughout this project with components of the code and our pleasant discussion.

Finally, I would like to thank my family and my fiance for their kindly support and love.

Table of Contents

Chapter 1

Introduction

Analyzing retinal vascular network changes of diabetes retinopathy (DR) patients help doctors diagnose the disease at early stages and make better medical treatment on patients. However, current diagnosis methods of DR requires long-term observation, which causes delay in individual clinical treatment. In this project, we employ graph theory and machine learning algorithms to explore features changes on DR patients to promote current diagnosis technology and make prediction on patients disease progression condition after a period of medical treatment.

1.1 Motivation

Inside the human body, thousands of arteries, veins and capillaries jointly compose the vascular system, which transport blood, oxygen and nutrient. This system clearly contains plenty of health information which could be vital to test the health condition of human body. Scientific research suggests that the retinal vascular system, which is one part of the vascular system, is the only part that can be assessed in vivo in human body, with the most clearness on observing and acquiring information [26].

Diabetes has been regarded as one of main threats of human health in the modern life. Patients with diabetes usually also have some symptoms on eyes such as like light loss and damage on retinal vessels, which reveals that retina and diabetes are related [22]. DR is a common complication of diabetes with symptom of large amount of retinal vessel damage on patient's eyes. However, it often too late to diagnose DR when patients' retinal vascular networks have significant changes. In this project, we regard human retinal vascular networks as research object and explore changes on DR patients retinal vascular networks from computational analysis aspects. Additionally, diabetes

treatment technique is crucial and we are still concerned about whether distinct therapy techniques can affect patient progression condition. The research aim is to give some suggestions for the medical institutions and hospitals to diagnose DR at early stages, to give better medical treatment choice, and to make prediction on individuals' disease progression to enhance public health.

1.2 Aims and Objectives

In this project, we employ graph theory and machine learning algorithms on human retinal network to detect the main differences between healthy people and DR patients. Similarly, we analyze changes on patients' eyes and the influence of different clinical treatment approaches during medical treatment period.

In this case, our first research objective is to propose a set of possible features which are noticeable among DR patients, along with mathematical modeling and computational representation by graph theory. What is more, after getting feature values, we implement features selection algorithm on the feature list to detect the main difference between healthy people and DR patients. Besides, given that we have patients medical treatment data, we explore deeper to find main feature changes as well as the difference of distinct treatment approaches after clinical treatment. Finally, based on above findings, we make prediction about patients disease progression condition after a period of medical treatment based on their initial retinal images.

1.3 Challenges

To identify correlations between retinal vascular system structures and diabetes, some particular challenges are narrowed down in this project:

- Data points are processed pictures that contain a lot of noise and information. In order to implement computational technologies on our dataset to get significant features from graph theory aspects, an efficient embedding technique for transferring pictures into graphs should be created, which is one of our main challenge;

- On the basis of embedded graphs, the most important research question is how to use graph theory techniques to identify valid and important primary characteris-

tics of the vascular network of patients. This requires large amount of biological background information and computational tests;

- Finally, with the reality that our information have been gathered and traced from actual patients, resulting in a restricted amount of information points, a fresh issue emerges: how can we make the most of these information and how to verify our results are sound is difficult.

The problem is challenging as it involves both biological concepts and mathematical modelling. However, we are able to obtain interesting results within a limited time.

1.4 Contributions

In this research, we propose three sets of metrics that can represent main features on retinal vascular network of DR patients: basic graph metrics, biological metrics and hierarchical ordering metrics. Those metrics show good performances to classify DR patients and healthy people, as well as detecting features changes during medical treatment.

- Basic graph metrics: they contain main features obtained by graph theory.
- Biological metrics: we build it biological and medical references with our mathematical modelling technology to describe the tortuosity of vessels, shapes of fovea and nutrition diffusion efficiency.
- Hierarchical ordering metrics: with intuitions from river network analysis, we propose the hierarchical ordering metrics which adapt faces (loops in graphs) merging orders as an effective way to compare structures of complex networks

Besides, we employ Bayesian logistic regression model to select important features when classifying healthy people and DR patients, as well as the medical treatment period, which gives some practical advice for doctors to diagnose DR at early stages and explore the changes during clinic treatment with accuracy of 70% and 87.33% separately. Finally, a "patient disease progression prediction" model has been provided with accuracy of 90.38% to make to help hospital make better medical suggestions for individual patients.

1.5 Overview of Paper

In this chapter, for the remainder of the document, we provide the fundamental overview of each chapter. In each section, we highlight the significant parts.

- **Chapter 2: Background** We provide the background context needed to comprehend our studies in the second chapter. We begin with introducing human vascular system and reviewing application of graph theory based on vascular network. Then, a short introduction of hierarchical ordering of vascular networks and diabetes risk score have been written to give readers some basic information about our methodology. Further more, we still add an short description of diabetes medical treatments that we are studying. Finally, the overview of our code structure is provided to help interested researchers to re-implement our project in a easy way.

- **Chapter 3: Dataset** In this chapter, we introduce our dataset and describe the preprecessing methods, as well as our data segmentation technology.

- **Chapter 4: Methods** This chapter is the most crucial part in this report. First, we make a description of feature metrics that we build to analyze DR patients' retinal vascular networks. Next, the methodology that we used to select significant features has been presented. The model employed to implement prediction task is in the final part.

- **Chapter 5: Results and Analysis** In this part, we explain the setup of our three experiments and present our results with tables and plots. We discuss the main features changes and provide some extra intuitions for clinical institutions based on our findings.

- **Chapter 6: Conclusion** We summarize our significant outcomes, examine our work's limitations, and give suggestion for future work.

Chapter 2

Background

Diabetes is a group of metabolic diseases characterized by hyperglycemia, which could lead to defects in insulin secretion, insulin action, or both [1]. In recent decades, the number of diabetes patients has increased significantly, which caused much more threats to public health. DR is a common complication of diabetes and it can be sight threatening. Current researches have proven that human retina imaging can be regarded as a source of biomarkers for diagnosis and prognosis of DR [26]. In this case, analyzing the differences of retinas between healthy people and DR patients is meaningful from clinical aspects.

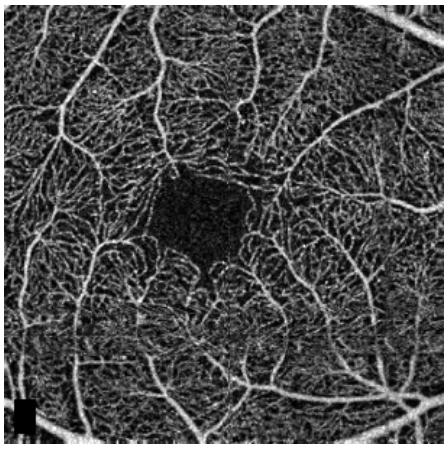

Figure 2.1: Example of healthy retinal vascular network.

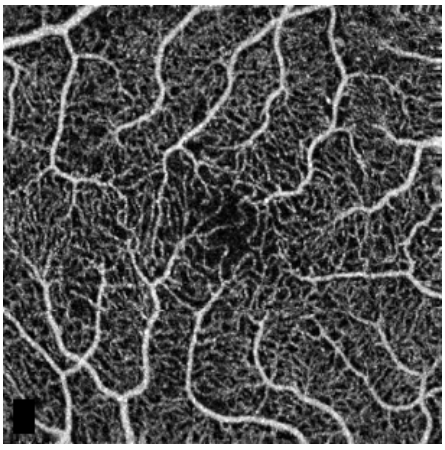

Figure 2.2: Example of diabetes vascular network.

Past study has discovered some important characteristics, such as fovea (the center pit in the eyes [15]) of patients with diabetes are usually irregular compared to healthy people [9]. However, since that vascular networks can be regarded as graphs, we propose an idea that there may be many other main features from graph theory aspects.

Those features may show good performance to classify healthy people from DR patients while they are not easy to be observed just by looking at images. In this project, we propose to use computational methods to detect and measure those features to help diagnose DR at the early stage.

Basal bolus therapy is one of the most common diabetes medical therapy techniques, while in latest days some fresh methods have been trilled in practical research to confirm that they have persuaded medical impacts on diabetes. Patients are handled in three distinct ways in our project. We should characterize what distinctions different clinical treatments make to the retinal network during the progression.

We also focus on the changes of features that we obtained during medical treatment period and make prediction for individuals based on their medical treatment data. In the future, when given enough amount of training data, we can use the patients baseline features to predict the medical treatment effect and give better suggestion about medical treatment.

2.1 Retinal Vascular Network

The vascular system is composed collectively within the human body by thousands of arteries, veins and capillaries, which attaches excellent significance to the transport of blood, oxygen and nutrition. There is certainly plenty of health information in this system that might be vital for testing the healthy condition of the human kind [26]. For our project, we plan to use the images of the retinal vascular network to be the evident object of the research, for the reason that the differences among different images could be easily detected in several perspectives.

2.2 Graph Theory Based on Vascular Networks

In recent years, graph theory has consistently been applied to giving complicated quantitative analysis on networks such as river system, which gives us intuition to apply it on networks within human body. With the fact that vascular networks' structural and functional systems have features of complex networks [5], there are still some work to implement the application. For instance, blood flow analysis has been adopted to detect the health condition of humans hearts and brains [32]; the distance among veins within the retinal vascular system have been measured to diagnose diabetes on rats [26]; also, other applications of graph theory on the retinal vascular network, such as

segmentation of optic disc and fovea, have revealed the usefulness of the graph theory [1]. Under the circumstance that the images of retinal vascular networks can be regarded as graphs due to their natural characteristics, we suggested that we should adopt the graph theory on analyzing the images, in order to figure out the principal difference between healthy people and DR patients.

2.3 Hierarchical Ordering of Vascular Networks

Spatial networks theory has been widely applied to biological systems [28]. For example, in leaf vein networks, side branching, which measures trees self-similarity value, has been widely used to measure structures difference based on spatial network theory [37]. In other biological systems, such as cardiovascular systems [16] and root systems [6], side branching theory has already been applied to analyze the networks' structure and function.

However, based on the fact that spatial networks are always complex, in fractal branching theory, we can make some simplification, for example, by dividing network into binary tree and detecting the topological structure of binary tree to measure the self-similarity of the original network. In this project, we use Horton-Strahler scheme [13] to get the hierarchical ordering tree of our retinal vascular network and analyze those trees to detect the structural differences between healthy people and DR patients.

2.4 Diabetes Risk Score

Risk score is a easy, practical and informative scoring scheme to quantify the risk value of diabetes-causing characteristics [24]. A factor is more vital for the model if it has a greater risk score value. What is more, factors with high risk score values can also be applied to make prediction of individuals' diabetes probability. A lot of machine learning algorithms, such as logistic regression, has been adapted to get the risk score and make prediction task [10].

In this project, we choose risk score as the tool to measure the importance of features that we obtained by implementing graph theory algorithms and comparing the importance the significant differences between the classification periods and medical treatment periods. The results will help to formalize the medical institutions about the effect of medical treatment and further treatment feedback.

2.5 Diabetes Medical Treatment

Successful treatment is the key factor for every patients long-term health, regardless their differences. For type 1 and type 2, the most important procedure is achieving balanced diabetes treatment. This project only involves with type 1 diabetes patients and their medical treatment methods could be categorized into three types:

- Insulin-Infusion-Pump Treatment: this method uses a small electronic device to provide diabetes patients with insulin needs and patients do not need to inject [36];
- Basal Bolus Treatment: this treatment requires patients to get regular injection per day before patients having meals. It is the most common treatment nowadays;
- Islet Cell Transplants Treatment: this treatment also require injection and has shown the effect of reduce the risk of severe hypoglycemic episode.

2.6 Implementation and Code

This project requires large amount of computational operation based on python. All scripts are in `.py` and `.ipynb` format. We set up several folders to manage the code scripts. The aim of this part is to help future students to find what they need or people who are interested in this area to re-implement the project and explore more.

The summary of our code is as following:

- Data: It contains raw data (`.png` OCTA retinal scan image files) and the summary of patients medical records that we got from doctors, as well as the preprocessed `.vtp` image files created by Ylenia as described in [2].
- Utils: This part is based on last year's MSc students and Dr. Bernabeu and Ylenia's code scripts [27] [3]. There are three main functions: importing `.vtp` files into graphs; data pre-processing and segmentation; finding faces in vascular networks.
- Metrics: All metrics that we proposed to measure the feature of the vascular networks are listed in this part. All scripts are written in `.py` format.

- Experiments: We designed a set of experiments to get the values of metrics for each image. Based on features' values, we implemented the classification and prediction tasks, and analyzed the importance of features as well as the visualization of features. All scripts are stored in python notebook.

- Results: All interim outputs like the simplified graphs and values of features, as well as the final results like the importance ranking and the prediction values are stored in this folder.

- Reports: This folder contains supporting materials such as plots and references which helps with our final reports.

Chapter 3

Dataset

In this part, we will discuss about our dataset and the preprocessing data technologies. As we have mentioned, our dataset are stored in `.vtp` files which contain much information like the coordinate of nodes, nodes radius and vessel thickness. Moreover, we have each patient's HbA1c [7] values during medical treatment, which provide information about the effect of medical treatment from sugar control aspect. We only have limited number of data points and some data points are not in good format, means that we need to handle with data sparsity and data missing problem, which increases difficulty in this project.

3.1 Data Overview

We have control group and DR patients group dataset in this project. There are 35 control images to give us information about features on healthy people's retinal vascular networks. As for diabetes data, we have 23 patients with images set and HbA1c values set, while each patient has 1 baseline data and several disease progression data in each set. Baseline is the moment when patients are enrolled in this study, while disease progression images are gathered when patients come to visit doctors during the treatment periods. Based on individual's health condition, doctor chose three medical treatment separately: pump treatment (IP), Basal Bolus treatment (BB) and Islet treatment (IT). There are 15 IP patients, 3 BB patients and 5 IT patients.

All patients should get screening of their retinal vascular network and testing of HbA1c value at month 1, 2, 3, 6, 9 and 12. However, since the facts that not all patients followed the instruction and, especially for the image set, some images are not in good quality, the diabetes dataset is incomplete. The example of patients image

medical records is as table 3.1 shows. The word 'MISS' means that the images are unavailable or the images are not in good quality. 'NULL' represents that patients did not visit the doctor to get regular check.

Patient ID	Baseline	Month 1	Month 2	Month 3	Month 6	Month 9	Month 12
IP08	09/01/18	06/03/18	MISS	MISS	17/07/18	MISS	MISS
IP09	17/01/18	05/03/18	12/04/18	11/05/18	09/08/18	12/12/18	30/01/19
IP10	03/07/18	MISS	MISS	MISS	MISS	MISS	MISS
IP11	20/07/18	MISS	MISS	09/11/18	27/02/19	NULL	NULL

Table 3.1: Example of patients physical check records.

As for the HbA1c value sets, we regard each patient's values change as the symbol of disease progression condition. If the HbA1c value decreases comparing with its last record, we assume that the patient's medical treatment works and the patient is getting better, as vice versa. By using 1 to depict patients getting better and 0 for worse, we produce disease progression labels for further analysis assignments.

3.2 Data Pre-processing and Segmentation

The OCTA retinal scans are converted to VTP files to divide vessels and background tissue [3]. The VTP images contain huge number of nodes and some noise which cause computational cost and inaccurate data analysis. In this case, importing VTP into graph and doing pre-processing is essential before implementing experiments.

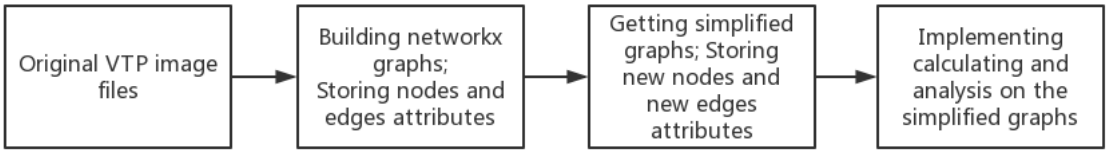

Figure 3.1: Data Preprocess diagram

3.2.1 Preprocessing

For the first step, we use python "Networkx" [12] package to build graph for each image. It provides effective network structure analysis functions which help us to

obtain the retinal vascular networks' features from graph aspects.

As we have mentioned, each image contains huge amount of nodes and noise, we implement the prepocessing process as following:

- Networking centering;
- Data cleaning by removing all nodes which have 0 degree;
- Data simplification by keeping the giant connected components and merging all nodes with degree of 2.

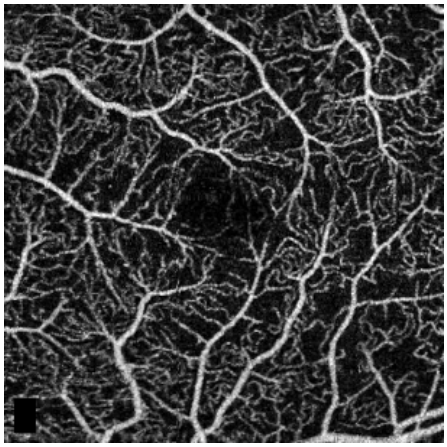

Figure 3.2: OCTA images.

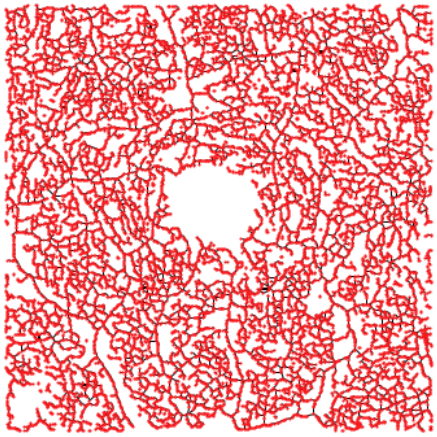

Figure 3.3: networkx.

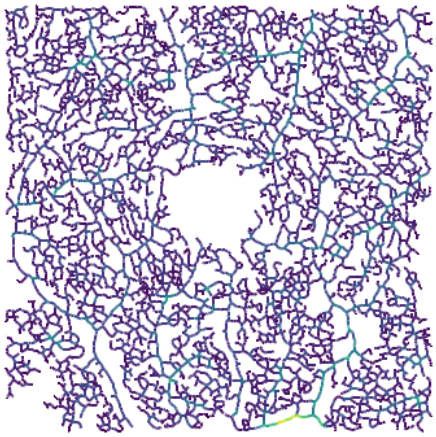

Figure 3.4: removed noise.

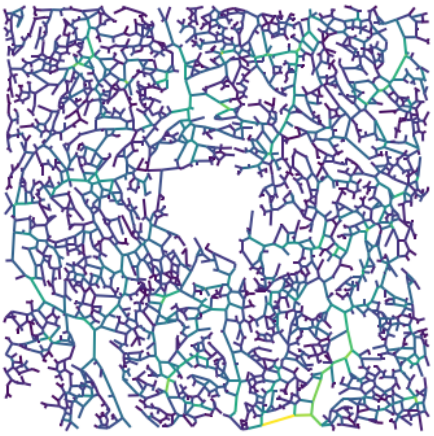

Figure 3.5: simplification.

Figure 3.2-3.5 show the changes of vascular network during the preprocessing process. The preprocessing tools were based on Rowen Sugden's code [35]. We still try several different methods like merging nodes based on angle or shortest path. However, due to the limitation of computational resource, the current simplification technology

has been adapted. All following experiments are implemented on the simplified graphs as figure 3.5 shows.

3.2.2 Data Segmentation

Current research has shown that the fovea parts and parafovea part have different functions and play distinct roles in human eyes [18], and disease can occur differently in distinct parts of those areas. It is reasonable that the vascular network changes are different. In this case, we divide our graph into 5 parts (as figure 3.5 shows) based on nodes coordinates. However, the segmentation method is not that accurate because it is just based on the coordinates of nodes, which may leads to imprecise results. In the future, this segmentation technology could be updated.

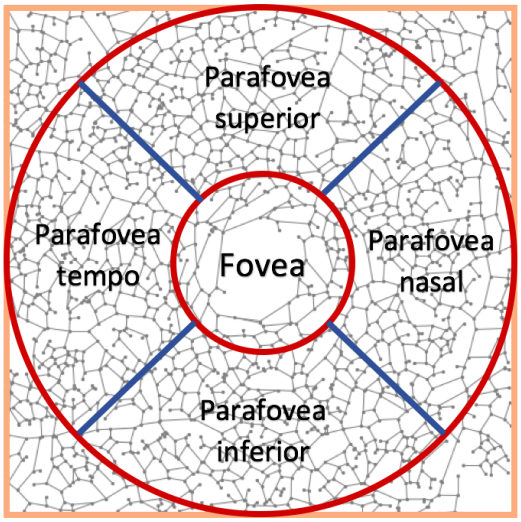

Figure 3.6: Retinal vascular network segmentation.[27]

Chapter 4

Methods

In this project, we want to detect the difference between healthy people and DR patients' retinal vascular networks. Moreover, since the medical treatment images have been provided, it is meaningful to explore network changes with different therapy methods. What is more, based on the fact that we have patients' HbA1c values which contains the information of medical treatment effect, we are expected to make prediction of individual's disease progression conditions.

Deep learning algorithms have shown powerful performance in biological area when given large amount of data points. However, based on the given dataset which only contains limited number of data, we cannot use deep learning methods which let the algorithm to detect useful features. In this case, we should propose a set of features from both biological and graph aspects and build the feature metrics to get the features' values.

After acquiring features values, we are still interested the importance of factors during the classification task (comparing healthy people and DR patients) and prediction task. In this case, we use machine learning algorithms to select the importance of features and leveraging the features that we have obtained to make prediction for each patients.

4.1 Feature Metrics

In this part, we use mathematical models to quantify the features of vascular networks. There are four kinds of metrics that we use:

- Basic metrics: Those metrics are based on graph theory, which represents each graph's basic properties.

- Biological metrics: Those metrics are built with medical references and doctors' experiences.
- Hierarchical ordering metrics: Those metrics analyze the topological ordering of the whole network. We get the intuition from similar network systems like river branch analysis and leaf vein systems.

4.1.1 Basic Metrics

All features in this part are acquired by implementing basic graph theory analysis. Disregarding the biological information, in this part, we just pay attention to retinal vascular networks' basic graph properties.

L2 distance: As we have mentioned in part 3, we have each node's coordinate information and we can get the L2 distances between every two nodes to evaluate the graphs' closeness.

Edge radius: We have the value of vessel radii from the VTP files. We describe the radius for each edge as the average of the radius at its two endpoints for algorithmic and visualization purposes [27].

Nodes density: Nodes density measures the number of nodes within a certain value of area. In this project, we regard each node as the center of circle and counts the number of nodes within radius of 1 to evaluate the density of nodes for every network.

Edge thickness: The VTP network were produced by nodes sampling, which means that in the original networks, the edges that we saw are actually the connection thousands of nodes as figure 4.1 shows. As the result, we use the average of nodes radius in the original network as the value of edge thickness.

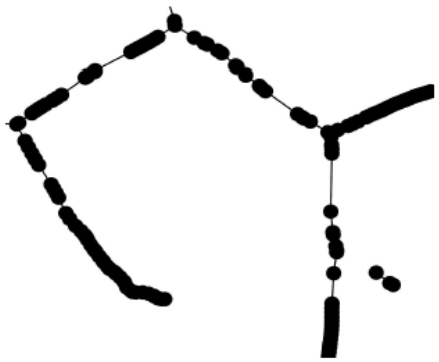

Figure 4.1: Detail of the original vascular network.[27]

Largest Laplace eigenvalue: Graph Laplace eigenvalues contain the spectral information [29] and has been adapted to many applications. We use the proportion of Laplace's biggest value as the metric in this project. In order to get the metric, we firstly get the adjacent matrix A and degree matrix D for each graph. The Laplace matrix L can be calculated as:

$$L = D - A$$

By calculating and ranking the eigenvalues of L, we can get each graph's largest Laplace eigenvalue.

4.1.2 Biological Metrics

In this part, we focus on the biological aspect information and use graph theory to quantify the biological changes. Previous medical research has proven that diabetes patients usually have irregular fovea shape and more curving vessel [23]. Besides, the nutrition diffusion efficiency is still diverse. Therefore, we propose three sets of metrics to measure the fovea shape, vessel tortuosity and nutrition diffusion efficiency.

4.1.2.1 Fovea shape measurement

Current research has shown that diabetes patient' fovea is more like a normal cycle or a normal oval while diabetes patient' fovea shape is much more irregular (as figure 4.2 and figure 4.3 show) [33]. In this case, we propose three "irregular" indexes to quantify fovea shape.

Before implementing the shape measurement experiments, we use the face finder algorithm to find individual's fovea zone. The term of face means the loop in graph. After detecting faces in each graph, we use python planar package to calculate the longest and shortest axis, perimeter and area of each face. The face with maximum area is exactly the fovea zone.

Axis Ratio: The ratio of longest axis over the shortest axis can represent the acircularity degree of an object[19]. Since the fact that if an object is a circle, the axis ratio will be 1. If the value of ratio is closer to 1, the acircularity degree would be lower. We use l_a to represent the length of the longest axis and s_a to represent the length of the shortest axis. The axis ratio(AR) calculating formula is:

$$AR = \frac{l_a}{s_a} \tag{4.1}$$

Circularity: Circularity is another index to measure object's circular with area and perimeter [20]. If the value is closer to 1, the object is more like a perfect circle. We use l to represent object's perimeter and s as the area, then the circularity (C) can be calculated by:

$$C = \frac{4 * \pi * s}{l^2} \tag{4.2}$$

Roundness: Unlike circularity using perimeter as denominator, we compare object's area with the square of longest axis to describe object's irregularity [19]. The roundness (R) can be calculated by:

$$R = \frac{4 * \pi * s}{{l_a}^2} \tag{4.3}$$

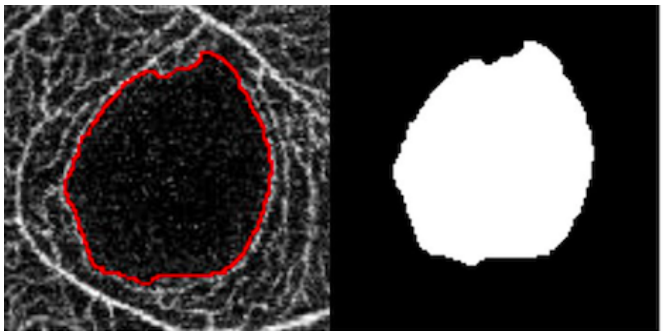

Figure 4.2: Example of healthy people's fovea shape.[33]

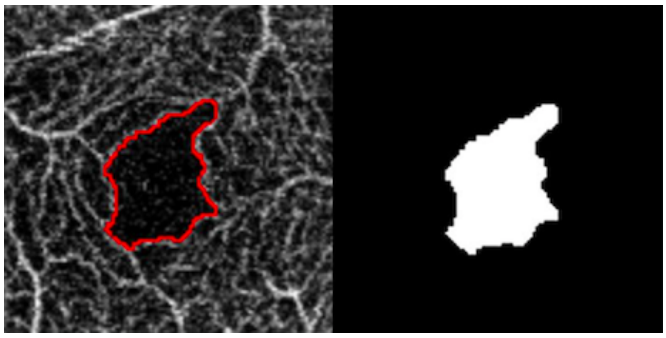

Figure 4.3: Example of diabetes patient's fovea shape.[33]

Those three features describe the degree of fovea shape from different aspects. The implementation code is in `fovea_shape.py` under the metrics folder.

4.1.2.2 Vessel tortuosity

Diabetes causes damage on human's vascular structure, which change the tortuosity of retinal vascular network [21]. Many tortuosity quantification methods have proposed

based on image pixel on conventional fundus photography [8]. However, most of the technologies are not that accurate and, in this project, we propose a new method based on our graph, which has better accuracy and results than traditional methods.

This method compares the original edges and the simplified edges in an single graph. As we have mentioned in chapter 3, we merge all nodes with degree of 2 on a single edge. As figure 4.4 shows, edge $ACDEFB$ is the original edge while during the simplification process nodes C, D, E and F were removed.

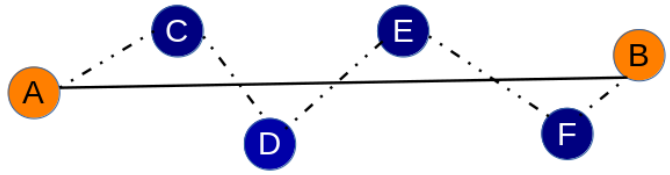

Figure 4.4: Example of original edge and simplified edge.

When calculating tortuosity, firstly we needs to get the values of the angles of every removed node with simplified edge like $\angle CAB$, $\angle EAB$ and $\angle FAB$, then getting the mean of absolute value of angles in each edge as figure 4.5 shows.

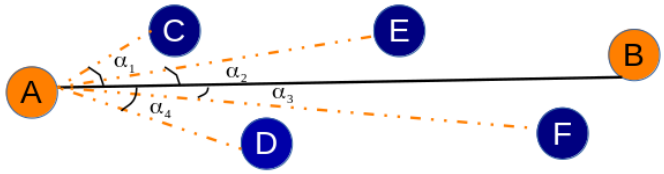

Figure 4.5: Example of edge angle.

Let n equal the number of removed nodes in each edge, we can give the calculation formula of tortuosity (T). If the edge is not curve, T equals to 0. If the value of T is large, the original edge is quiet curve.

$$T = \frac{\Sigma|\alpha_i|}{n} \tag{4.4}$$

4.1.2.3 Area to Perimeter ratio (A2P) Value

Because diabetes causes harm to the vascular structure of patients, which affects the efficacy of diffusion of nutrition within human body. Current research has shown that

there is some significant efficiency difference in lung and kidney vascular system [30]. This gives us intuition to detect the differences in retinal vascular systems.

A2P is shorted for "Area to Perimeter ratio" [35] to measure the diffusion efficiency to the surrounding tissue in mouse retinal vascular network [27], while this project, we apply the algorithm on human dataset. The algorithm is based on faces (as figure 4.6 shows) which means loops in network.

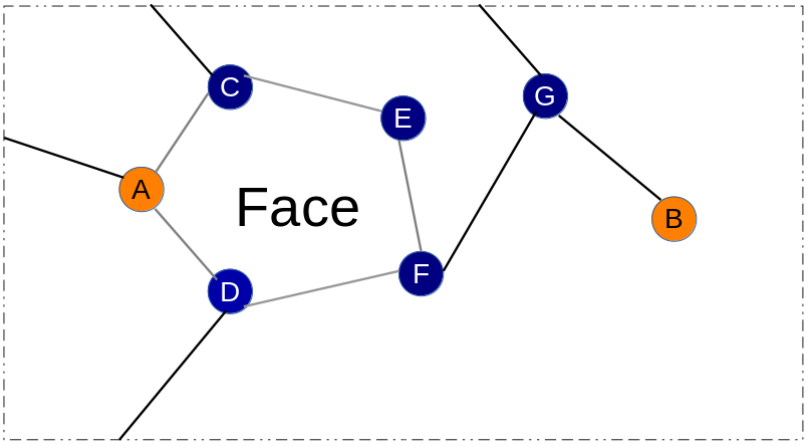

Figure 4.6: Example of face in vascular network.

If we regard edges as vessels, since we know the thickness and length (L2 distance) of each edge, we can evaluate the amount of transporting nutrition in each vessel by multiplying its thickness and length. The target tissue's nutrition amount can be estimated by the area of face. By comparing the nutrition in surrounding vessels and face, we can evaluate the diffusion efficiency of vascular network. Supposed that s means the area of face, d_i and t_i means the L2 distance of thickness of vessel that surrounds the face, the calculating formula is as following:

$$A2P = \frac{s}{\Sigma id_i * t_i} \tag{4.5}$$

4.1.3 Hierarchical Ordering Metrics

When analyzing complex networks, how to design an effective and accurate structure analysis algorithm is crucial. [5] Since the face that complex network like biology system and river system have large amount of nodes and randomness, which requires heavy computational cost, it is impractical to implement traditional graph structure analysis on those complex network.

In river system networks, scholars have employed the information of hierarchical

ordering to compare the structure similarity among different graphs [28]. Generally, the ordering algorithm is based on Horton-Strahler scheme [34].

In this part, we apply the river hierarchical ordering algorithm on retinal vascular network to analyze the structure of biological network. This algorithm is based on faces and weighted edges in networks as figure 4.7 shows. In this part, we regard the vessel thickness values as weights. We get the topological ordering of each graph by merging faces and the merging ordering scheme is based on the weight of edges [17].

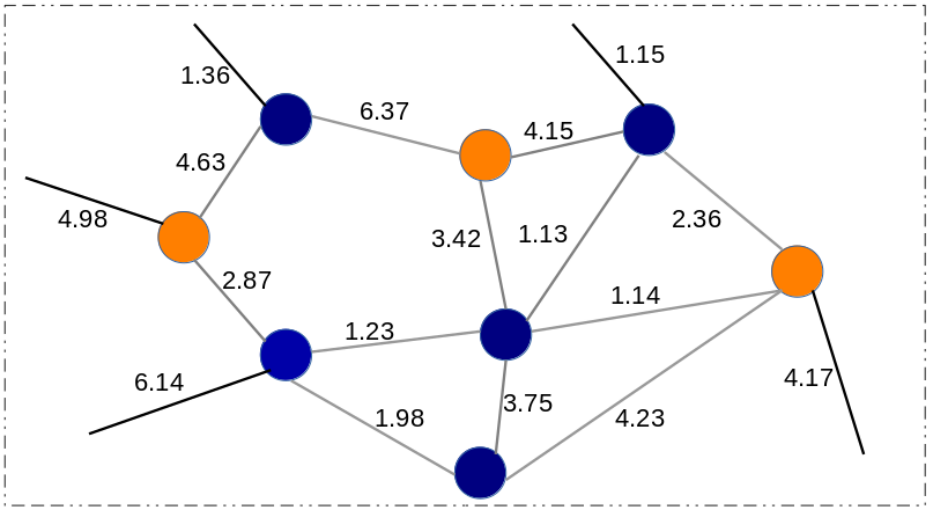

Figure 4.7: Example of faces with weighted edges in vascular network.

We use the thickness of edges as the weight index. The reason why we choose thickness is that, from biological aspect, thickness contains the ranking of vessels. My peer Alisa also tries L2 distance as weight index.

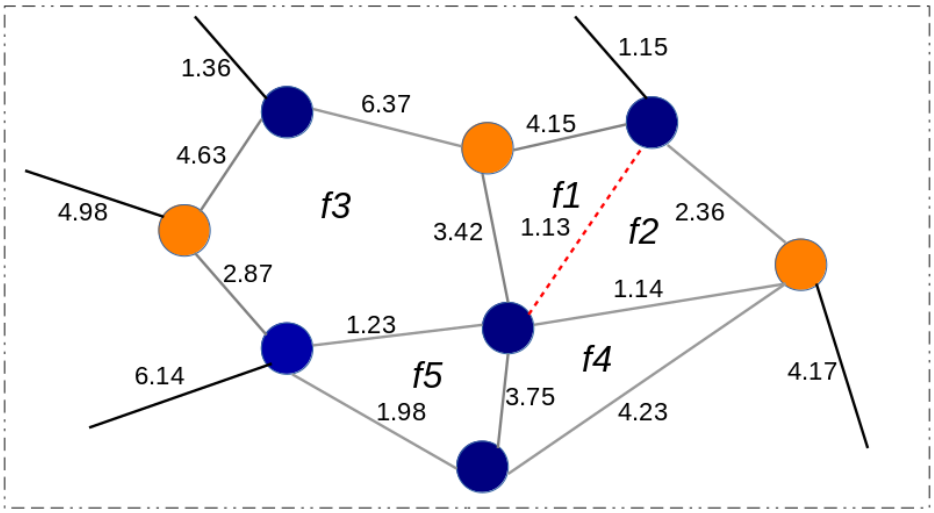

Figure 4.8: Example of faces merging order.

At the beginning points, we assign each face with wight 1. Then we begin to search all edges and break the lightest edge and update faces weights at the same time. The searching algorithm ends when there are no faces in each network. Figure 4.9 explains the example of network after removing loops. At the same time, we can get the faces merging order tree as figure 4.10 shows. In figure 4.10, the blue nodes have weight 1, orange nodes have weight and purple nodes with weight 3.

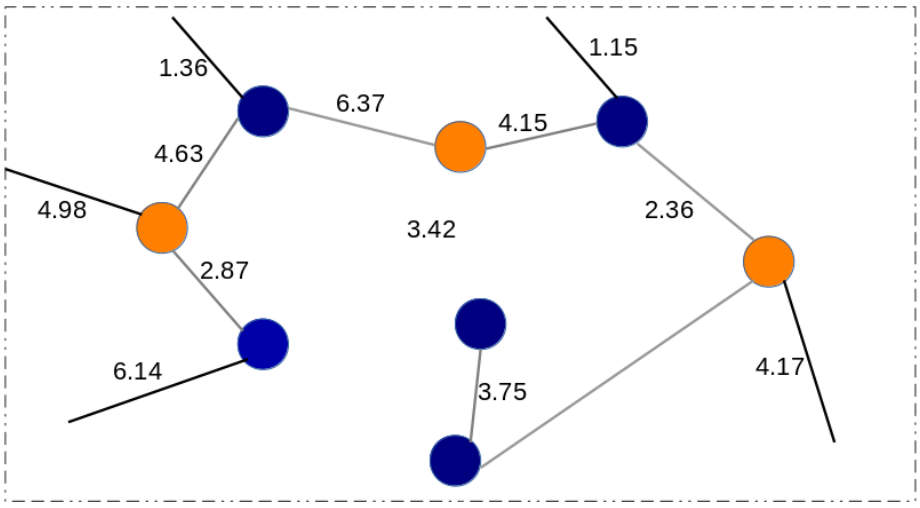

Figure 4.9: Example of merged graph without faces.

When given a loopy graph, by implementing the following algorithm, there are two outputs: the face merging order tree and the merged graph without loops.

- Input: Retinal vascular network;
- Getting the number of faces n, faces list and edges weight list;
- Assigning each face with weight $\lambda_i = 1$;
- Finding the lightest edge e_{l1} and the two faces f_m and f_k that e_{l1} belongs to; removing e_{l1} and adding the new merged face f_{mk} to faces list. The weight of f_{mk} can be calculated as:

  if $\lambda_m = \lambda_k$, $\lambda_{mk} = \lambda_m + 1$;

  if $\lambda_m \neq \lambda_k$, $\lambda_{mk} = max(\lambda_m, \lambda_k)$
- Keeping update the faces list and faces weights until there are no faces in the network.

In this project, we only pay attention to the faces merging tree (as figure 4.10 shows). We propose three structural metrics to describe the tree from several aspects. By comparing the value of above three metrics, we can get the structural features of the original loopy graphs.

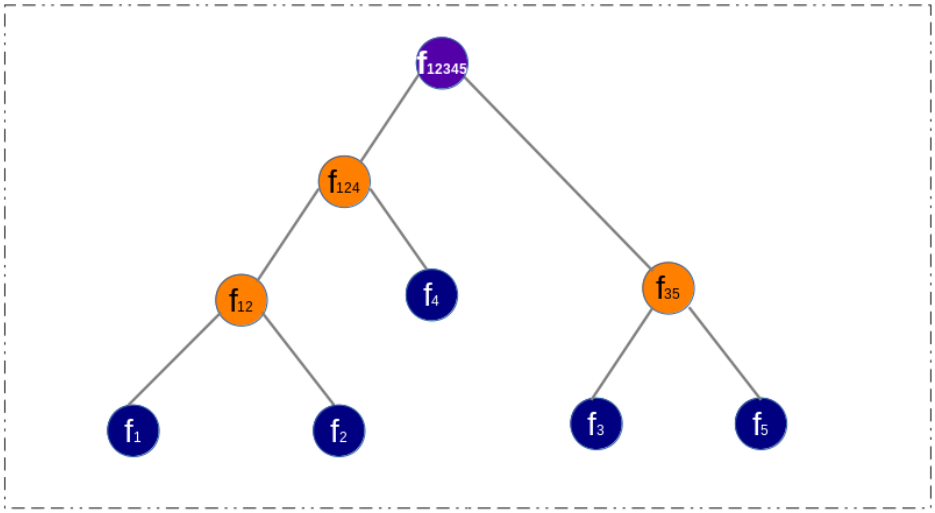

Figure 4.10: Example of faces merging order tree.

1 Side branching value

Before giving the definition of side branching, we first explain some mathematical notations that will be employed:

- N_{ij}: the number of j order branches flow into j order branches.

  In figure 4.10, for example, $N_{1,2} = 5$ because the number of $1-$order branches flowing into $2-$order branches (f_1 to f_{12}, f_2 to f_{12}, f_4 to f_{124}, f_3 to f_{35} and f_5 to f_{35}) is 5.

- N_i: the number of other order branches connecting to $i-$ order branches.

$$N_i = \Sigma_j N_{ij} \tag{4.6}$$

  In figure 4.10, for example, $N_2 = 8$ because $N_{1,2} = 5$, $N_{2,2} = 1$ and $N_{3,2} = 2$, in this case, $N_2 = N_{1,2} + N_{2,2} + N_{3,2} = 5 + 1 + 2 = 8$.

The side branching value [31] , which defines the self-similarity of tree, has been widely used in river system network. The calculation formula of side branching value R is as following:

$$R = \frac{N_i}{N_{i+1}} \tag{4.7}$$

From the definition, we know that the side branching value reflects how the tree growth. If the ratio of 4-order to 5-order is quiet similar to the ratio of 1-order to 2-order, we can infer that the tree grow with fixed extension value.

2 Inner percentage (RI)

Here we pay attention to the nodes with weight 1. Since the fact that the 1-order nodes have the accounts for the largest percentage in the binary tree and their positions are always in the inner part, we define this metric:

$$N_{in} = \Sigma_j N_{1,j} \tag{4.8}$$

$$RI = \frac{N_{in}}{N} \tag{4.9}$$

3 Outer percentage (RO) Similarly to the inner percentage, the outer percentage also describe tree structure from detailed aspect. Here we pay more attention to the max order nodes and they are always at the outer part of trees. For example, in figure 4.10, the max weight is 3. We give similar definition as inner percentage:

$$N_{out} = \Sigma_j N_{max,j} \tag{4.10}$$

$$RO = \frac{N_{out}}{N} \tag{4.11}$$

In summary, when given a complex network, instead of analyzing the network itself, we get the structural information by implementing algorithms on the graph's faces to get topological ordering information including side branching value, inner percentage and outer percentage.

4.2 Risk Score and Feature Selection

Several recent intervention studies have shown that people can efficiently prevent diabetes by changing their lifestyle [11] [14]. And in their studies, risk score has been widely used to measure the importance of factors like gender, age, diet and so on [24]. Some machine learning algorithms like KNN, decision tree and support vector machine (SVM) have been widely applied to classify healthy people and DR patients. In most cases, logistic regression was employed to compute the coefficient β_i which produces the values of risk score. x_i represents value of feature and $logistic(y)$ is the classification label.

$$logistic(y) = \beta_0 + \beta_1 x_1 + ... + \beta_n x_n \tag{4.12}$$

This leaves us an intuition that we can apply the risk score algorithm on our dataset and get the importance of changes on the retinal vascular network. After getting the risk scores of our features, we rank the importance of features based on the value of coefficient β_i .

Since the fact that the number of data points are limited, in order to increase accuracy, we add Bayesian feature selection in this part [25]. In this case, we use the Bayesian logistic regression model to estimate the value of β_i. Supposed that the prior information is that:

$$\beta \sim N(0, \sigma^2 I_n) \tag{4.13}$$

Then we can write our likelihood as:

$$y_i \sim N(0, \beta^T x_i \sigma^2) \tag{4.14}$$

So, the distribution of $(x, y|\beta)$ can be represented as:

$$p(x_i, y_i|\beta) \propto N(0, \beta^T x_i \sigma^2) \tag{4.15}$$

By multiplying the likelihood and prior information, we have the representation of posterior:

$$p(\beta|x, y) \propto p(x_i, y_i|\beta) p(\beta) \tag{4.16}$$

In this case, we get the estimation of β by using the dataset (x, y) and use the normalization value of β to represent each features' risk score value.

4.3 Prediction

Predicting individuals disease progression has been regarded as a crucial task. Although this task is quite meaningful, accurate prediction is always hard to make. As we have mentioned, the data points in this project are limited, which means that it is hard to get general conclusions. Although the limitation is obvious, it is still meaningful to analyze individual's dataset and give some intuitions to future research with large amount of data.

In this project, our dataset has been divided into two parts: classification part and medical treatment part. We only make predictions on the medical treatment part with

the aim of giving better medical treatment suggestion to individuals. We still use the logistics regression model to make predictions, and the algorithm is as following:

- Fitting the LR model:

$$f(x) = \Sigma\beta_i x_i, i = 1, 2, ...n \tag{4.17}$$

- Ranking features, dropping all ineffective features and producing new LR model:

$$f_{new}(x) = \Sigma\beta_i x_i, i = 1, 2, ...m(m < n) \tag{4.18}$$

- Inputting data and make prediction by $f_{new}(x)$.

The feature selection and prediction codes are stored in the "Experiments" folder. Based on different task aims, we have designed a set of experiments to analyze the dataset.

Chapter 5

Results and Analysis

In this part, we are going to describe our results and analyze the main findings. We use accuracy to evaluate our models performance and it is defined as the percentage of size of right classification set over the entire set. Higher accuracy value means better performance. All models are estimated by the "5-cross-validation" algorithm. In the first step, we employ preprocess and segmentation on all images, following by implementing metrics on the processed dataset. After obtaining values of features, there are two main objects in this projects:

- **Classification**: Detecting significant features that can classify baseline patients and healthy people. In the classification task, we design a experiment to compare control images and diabetes baseline images. Our model gets the accuracy of 70% by "5-cross-validation" algorithm.

- **Prediction**: Detecting significant features that can predict patients' disease progression, as well as employing the detected features to make future predictions.In this part, we acquire a set of important characteristics and visualize changes on those characteristics by training our model with baseline pictures to predict the disease progression on month 1. Moreover, we combine baseline pictures with month 1 or month 3 information together to see if forecast precision improves. We get accuracy of 87.34% in the prediction task of month 1, along with 90.38% accuracy by using baseline and month 1 images predict month 3.

When obtaining features values, the side branching, inner percentage and outer percentage metrics are implemented on whole networks without segmentation, since the structure information can be better reserved in this way. Other metrics are implemented on the segmented dataset. Each feature may contain more than one value, for

example, we have A2P mean, median, variance, skew and kurtosis values to implement analysis. After implementing all metrics that we have proposed, each image has six sets of feature as table 5.1 shows. The reason why we analyze the features on different set is that some features may be important on some sets while they may not significant on other sets. In this way, we can give better suggestions to doctors to detect further biological meanings in the future.

Set	Fovea	Nasal	Tempo	Superior	Inferior	Structure
Feature List	Roundness Axial Ratio Circularity A2P L2 distance Thickness Tortuosity Radius Laplace value Nodes density	A2P L2 distance Thickness Tortuosity Radius Laplace value Nodes density	A2P L2 distance Thickness Tortuosity Radius Laplace value Nodes density	A2P L2 distance Thickness Tortuosity Radius Laplace value Nodes density	A2P L2 distance Thickness Tortuosity Radius Laplace value Nodes density	Side branching Inner percentage Outer percentage
122	26	23	23	23	23	3

Table 5.1: Feature list: each feature contains at least one value.

5.1 Classification

In this task, our research goal is to detect significant differences between healthy people and DR patients. In the first experiment, there are 35 healthy people's retinal vascular network and 23 patients' baseline images. We firstly add labels to each image. If the image comes from healthy people, the value of label is 0; if it is a baseline image, the label will be 1. We use "5-cross-validation" [38] algorithm to evaluate our model by randomly selecting 80% of our dataset as training set and 20% as test set.

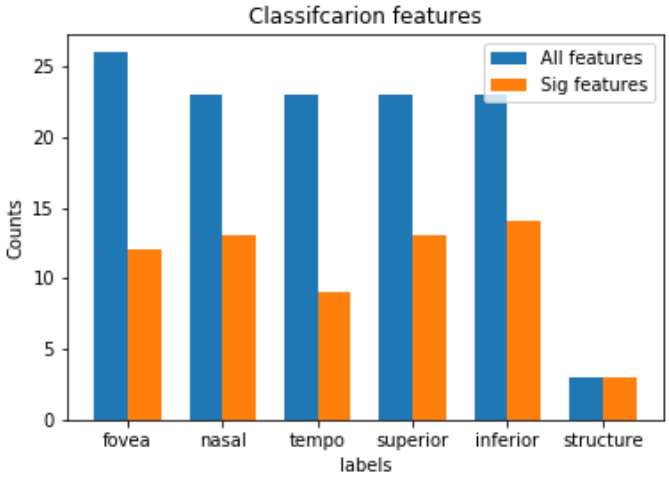

Figure 5.1: Significant features distribution in different parts of retinal vascular network in the classification task.

5.1.1 Results and Evaluation

We repeat the "5-cross-validation" algorithm on our dataset for 5 times and use the average value as the final accuracy. The final accuracy is 70%. Since that our dataset is limited and there may be some outliers, the performance of our algorithm is well. In this case, we can use our trained model to get the risk score of every features.

We first evaluate all β_i's p value by statistics test and remove all insignificant features. Then we assign every feature with a risk score based on the value of β_i. The significant features and their risk scores are in table 5.2.

5.1.2 Discussion

First, we compare the importance of different parts. From figure 5.1, we can find the distribution of important features: structure, fovea and inferior parts have most important features, which means that when getting new images from doctor, we can firstly analyze those two parts if we have limited computational resources. There are some other information noticeable:

- **Tortuosity is important on almost every part.** From table 5.2, we can find that tortuosity has been regarded an significant feature on fovea, inferior and nasal parts. Besides, the mean value of tortuosity is also important on superior and tempo part. The results has verified the biological reference that vessel curve

Feature	Coefficients	Risk Score
Outer	-2.714e-07	3
Inner	-1.42e-08	1
Side Branch	9.036e-07	9
Fovea Circularity	-3.674e-07	4
Fovea Axial Ration	-9.359e-07	7
Fovea Roundness	-1.19931e-05	10
Parafovea Nasal A2P	-1.72e-08	1
Parafovea Nasal L2 distances	-3.86455e-05	10
Parafovea Nasal Tortuosity	-1.1185e-06	10
Parafovea Inferior A2P	-1.37e-08	1
Parafovea Inferior L2 distances	-4.11854e-05	10
Parafovea Inferior Thicknesses	-0.0011139407	10
Parafovea Superior Tortuosity	-2.0347e-06	10
Parafovea Tempo Radius	-1.67141e-05	10
Fovea A2P	-1.72e-08	1

Table 5.2: Significant features risk score in the classification task. Note: each feature has 5 values like mean, median and so on, and we only list features that at lease three values have been regarded as significant in this table.

changes happens patients retinal vascular network. In every part of retinal vascular network, patients vessel tortuosity is higher than healthy people.

- **The order of face merging is important.** As we have mentioned in the methodology part, side branching describes an average growth of the face merging binary tree. The fact that side ranching value has been regarded as significant factor reveals that patients network structure has notable differences from macroscopic aspects. This result guides us that it is valuable to explore more on the structure of retinal vascular networks like persistent homology [4] in the future works.

- **Fovea shape contains people's healthy information.** Fovea axial ratio and roundness are also in the significant list, which also verifies the biological reference that diabetes patients have more irregular fovea. From figure 5.2 we can see that in control group, the log 10 mean value of axial ratio is around 0 and the mean value of roundness is 1, which has similar value with perfect circle. While

in patients group, the ratio is larger and roundness is smaller, which means that patients fovea is usually not that a round.

Apart from above findings, we also know that the vessel thickness is a noticeable feature. Besides, the appearance of A2P value verifies the fact that DR patients' nutrition diffusion efficiency is significantly affected by the disease. In addition to figure 5.2, we also have other parts box plots which show the statistics differences of significant features for the classification task and they can be found in the appendix part.

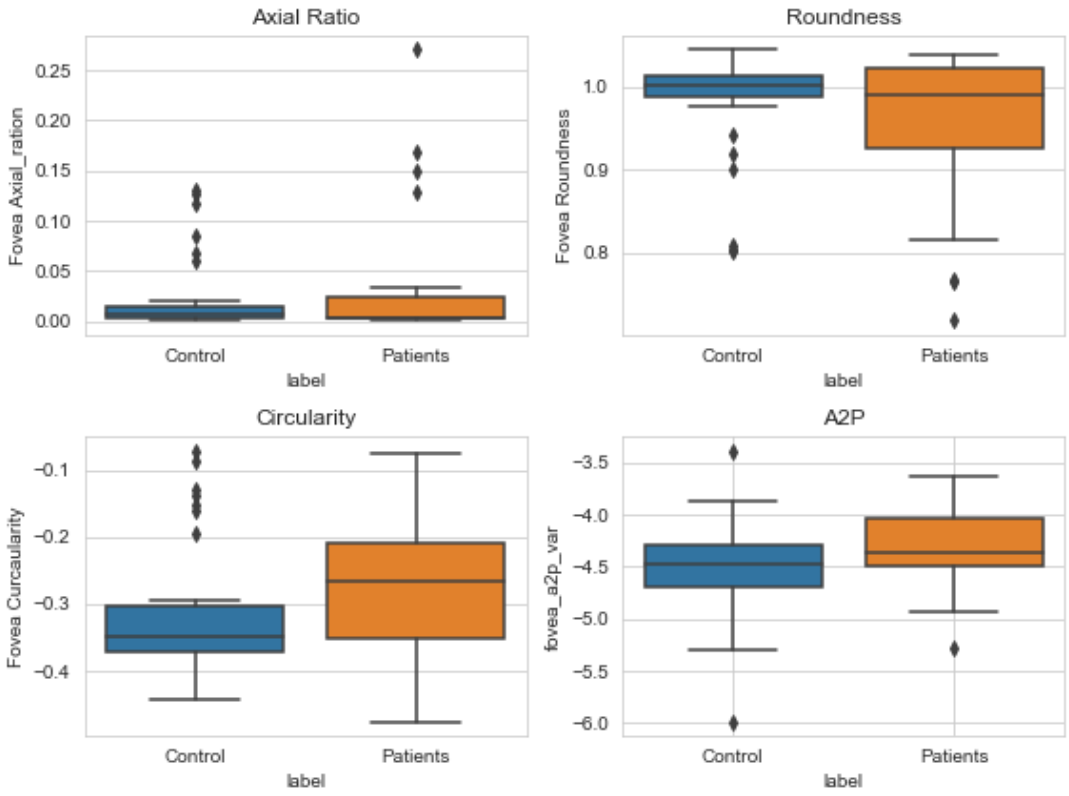

Figure 5.2: Fovea changes in the classification task: healthy people have higher values of axial ratio, circularity and A2P and lower value of roundness.

5.2 Prediction

In this part, we design two sets of experiments to detect important features and make predictions. For the first set, we want to get significant features and visualize changes in those features by training our model with baseline images to predict the development of the disease on month 1. In the second part, we combine baseline images with month 1 or month 3 data together to see if prediction accuracy is improving.

5.2.1 Month 1 Prediction

In this case, we have only 23 patients in the dataset and we use the values of the features on the baseline image as inputs for each patient. Since the patients were treated in distinct medical techniques, we add the "medical treatment" feature in the characteristics list: if a patient uses insulin-infusion-pump treatment, the "medical treatment" value is 1; basal bolus Treatment and islet cell transplants treatment get the value of 2 and 3 separately.

As for label, we use each patient' disease progression labels that we defined in chapter 3 based on HbA1c values change. The evaluation algorithm is the same as the classification task with "5-cross-validation".

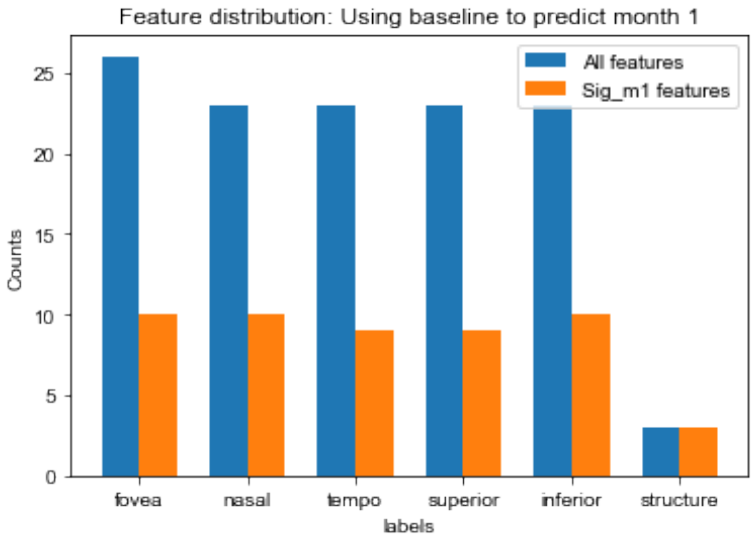

Figure 5.3: Features changes distribution in the month 1 prediction task.

5.2.1.1 Results and Evaluation

By implement the evaluation task, the average accuracy is 87.34%, which shows that our model is convinced on the given dataset so that we can implement further analysis on features. We can find the distribution of significant features on figure 5.3 and the risk score in table 5.3. Same as the classification task, we only list features that at lease three values have been regarded as significant to show the importance of features in the list.

Feature	Coefficients	Risk Score
Treatment	1.6e-09	1
Outer	2.1e-09	1
Inner	4e-10	1
Side Branch	-1.1e-08	1
Fovea Axial Ration	2e-09	1
Parafovea Nasal A2P	1.408e-07	10
Parafovea Inferior L2 Distances	8.502e-07	10
Parafovea Superior A2P	-3.84e-08	4
Parafovea Tempo A2P	-3.9e-08	4
Fovea L2 distances	1.371e-07	10

Table 5.3: Significant features risk score in the month 1 prediction task. Note: each feature has 5 values like mean, median and so on, and we only list features that at lease three values have been regarded as significant in this table.

5.2.1.2 Discussion

From figure 5.3, we can find that, comparing with figure 5.1 which shows the distribution of significant features in the classification task, the number of important features decreases in every part. There are 12 significant features on fovea part by comparing the baseline images and control images, while only 10 features show significance in the medical treatment period. Same things happen on other parts of the network.

The decrease of features' number reveals us the information that there are some features that are hard to change with short term medical treatment. This is reasonable because from some references we know that diabetes patients are hard to be recovered since there are not much effective medicines to defeat this disease. There are still some other noticeable findings which can give some intuition to medical researches:

- **The choice of medical treatment is important.** As we have mentioned in the background part, there are several kinds of medical treatment methods and each of them has obvious benefits and drawbacks from practical aspects. For example, insulin-infusion-pump treatment dose not require patients to get injection, which may be good for children patients. However, since the fact that medical treatment has been regarded as a significant feature by the algorithm, it shows that the effect of different medical treatments varies during the first month treatment. It

may be true that some medicines may employ quick effects on patients which can help doctors to control patients condition in short time. In this case, we would make an inference that the choice of medical treatment is crucial for patients.

- **The topological structure of retinal network is sensitive to small changes.** Figure 5.4 shows that changes of mean values of outer percentage, inner percentage and side branching percentage from month 0 (baseline) to month 3. Those three features all show significance in the classification task and month 1 prediction task, which tells us that the order of face merging is a good index to measure the changes of retinal vascular network.

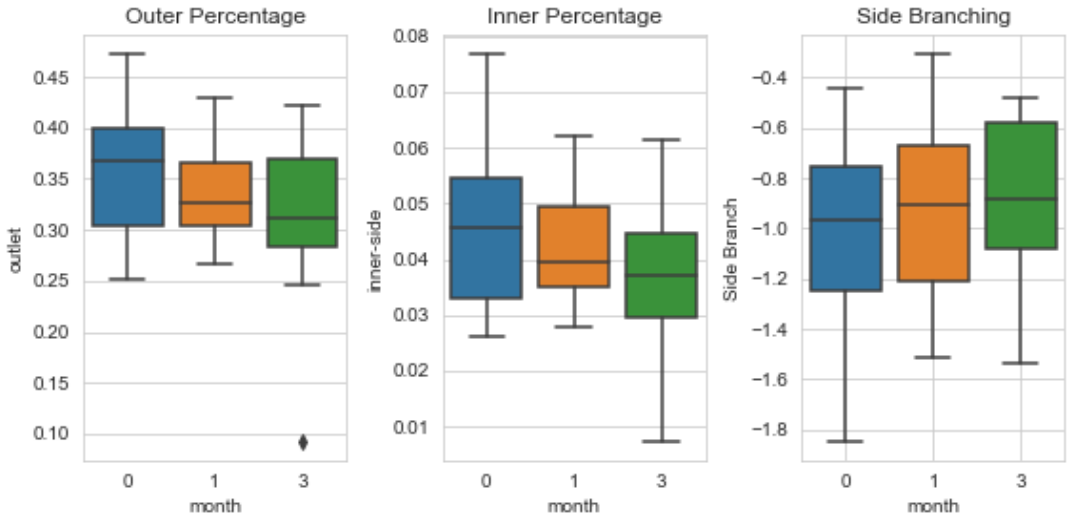

Figure 5.4: Structure changes on baseline, month 1 and month 3: outer and inner percentage values drop while side branching value increase during medical treatment.

As time goes by, the outer percentage and inner percentage decrease, which means that the binary trees become more and more like a complete tree. The absolute value of side branching decrease, shows that the binary tree grows slower in length while faster in width, which also verifies the conclusion we got from outer percentage and inner percentage.

- **Fovea shape changes features play different roles.** In the classification period, all three fovea shape features are important to classify healthy people and DR patients, while only axial ratio shows significance in the month 1 prediction. We use log function on the fovea axial ratio values and if the value is closer to 0, the object is more like a perfect circle. Figure 5.5 reveals that the value of axial ratio

drops from baseline to month 3 and it is more and more close to 0. This gives us the intuition that axial ratio may be easier to change comparing with roundness and circularity.

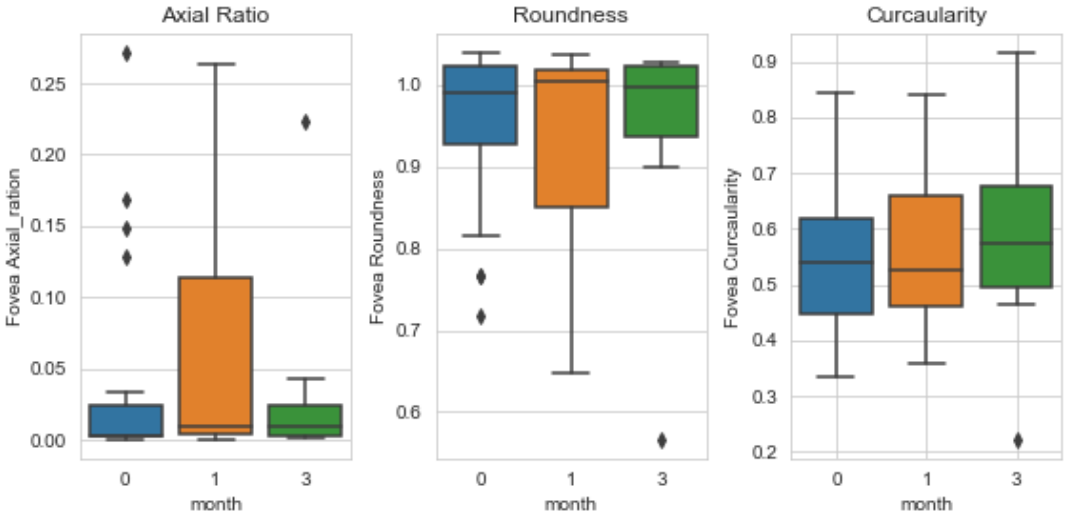

Figure 5.5: Fovea shape changes on baseline, month 1 and month 3: axial ratio decreases while roundness and circularity increase.

Roundness reflects the irregular degree of objects while it is not sensitive to boundary shape. We can find that after three month treatment, the value of roundness has been around 1 (which is the value of perfect circle). Circularity can represent the shape of objective boundary and if the value is 1, the boundary is quiet smooth. From figure 5.5 we can see that although there is a small drop on month 1, the value of circularity increases slowly. Combining the three values, we can find that medical treatment first changes the shape of fovea from macroscopic aspect by shorting the difference of long axis and short axis while the recover of boundary requires long term treatment.

- **Medicine actually changes the diffusion efficiency.** From table 5.3, we can find that A2P is significant in almost every part of eyes, which verified our biological references that diabetes patients cells diffuse slower comparing with healthy people. This gives us intuition that we can build more accurate model on the A2P features in the future work since it may be able to capture small changes which happen at early stage of diabetes.

We still have other parts box plots which show the statistics differences of significant features for the month 1 prediction task and they can be found in the appendix

part.

5.2.2 Further Prediction

In this assignment, by combining their baseline picture and month 1 or month 3 pictures, we create further predictions on diabetes patients about their disease progression situation. In the assignment of month 1 prediction, we discover that baseline pictures can provide vital data to forecast development of disease in patients. In this situation, if we have more data like month 1 and month 3 picture, can we create better prediction?

5.2.2.1 Experiments

Same as the month 1 prediction part, we employ the disease progression labels as our training label. We design 3 experiments to make prediction:

- Month 3 prediction: Similar like Month 1 experiment, in this case, we use baseline images and month 3 disease progression label to make prediction;
- Further prediction based on month 1: Instead of only using the baseline images, in this experiment we make prediction based on patients baseline and first month images, and make prediction for month 3 and month 6;
- Further prediction based on month 3: Similar like experiment 2, in this case, we regard baseline and month 3 images as inputs and make prediction on the treatment condition afther 6 months medical treatment;

We still use Bayesian logistic regression model and the "5-cross-validation" algorithm to evaluate the model's performance.

5.2.2.2 Results and Discussion

By repeating the "5-cross-validation" algorithm for 5 times, we get our results as table 5.4 shows. We use the mean value as the final results. To create a clear comparison, we add the outcome of the month 1 forecast to the table. Most of the accuracy values are quiet high, suggesting that our models performed well in the prediction tasks. However, due to that we only have limited number of data, whether our algorithm can be employed on larger dataset requires further discussion.

From the above table, we can find some noticeable results which may give doctors intuition in the future work:

Training		Prediction Accuracy		
Train Image (X)	Disease Progression labels (Y)	Month 1	Month 3	Month 6
Baseline	month 1 vs baseline	87.34%	/	/
Baseline	month 3 vs baseline	/	66.67%	/
Baseline and month 1	month 3 vs month 1/ month 6 vs month 1	/	90.38%	87.58%
Baseline and month 3	month 6 vs month 3	/	/	63.67%

Table 5.4: Prediction accuracy results on the disease progression of month 1, month 3 and month 6

- Comparing with the first and second rows, the model is more accurate to predict the short time recover condition (with accuracy of 87.34% on month 1) than longer time recover (with accuracy of 66.66%). The results also tell us that the patients' baseline images contain information that the difficulty of getting recovery and doctor adjusts patients medical treatment methods based on the prediction.

- Comparing with the second and third rows about prediction of month 3, we can find that given the information of baseline and month 1, it is easy to make inference of recovery condition of month 3. This is reasonable since the second experiment contains more information about individual health condition.

- Comparing with the third and last rows about prediction on month 6, we find that the information of month 1 is crucial. Given baseline and month 1 information, the prediction accuracy is much higher that information of baseline and month 3 (87.58% and 63.67% separately). This gives us some intuition that first month medical treatment must be one of the most crucial part and the recovery degree on month 1 has high probability to influence patients' long term treatment results.

Chapter 6

Conclusions

In this project, our research object is human retinal vascular network and we employ graph theory to analyze changes happening at DR patients retinal vascular networks. In order to quantify features changing, we proposed a set of metrics and implemented the metrics on retinal of healthy people and DR patients. Based on our metrics, we implemented a set of analysis tasks.

6.1 Brief Summary

In general, our main conclusions come from the following three tasks:

- **Classification Task**: In this task, we analyzed the main differences of retinal vascular network between healthy people and DR patients. From the significance of features, we know that changes on the vessel tortuosity, A2P value (revealing the nutrition diffusion efficiency) and fovea shape are noticeable on DR patients retinal vascular network. Besides, from the graph theory aspect, the order of face merging also can also be regarded as a good index to diagnose DR at early stage.

- **Month 1 prediction**: By detecting noticeable features that influence month prediction accuracy, we find that the choice of medical treatment is important because it influences patients' the disease progression significantly. Besides, since the fact that the face merging order features (side branching, outer and inner percentage) show significance both in the classification task and medical treatment period, we therefore draw a conclusion that topological structure of retinal network is sensitive to small change. What is more, it is noticeable that patients'

axial ratio will firstly get recovered, then the roundness, and finally the circularity which reflects the boundary irregularity during the medical treatment.

- **Further Prediction**: We implemented 3 experiments to predict individual's disease progression after a period of medical treatment. We find that it is possible to use baseline images to make inference of disease development after one month treatment. Results also reveal that first month medical treatment is crucial because it can not only provide much information about long term medical treatment result prediction, but also influences patients final recovery results.

6.2 Limitation and Future Work

Although our project shows great results and reveals much information to biological research, there are still some limitations. We list the limitation and give suggestions to future work:

- Accuracy of data segmentation: in the data segmentation part, we just use nodes coordinate to make segmentation, which produces influences on the detection of fovea and final results. Therefore, in the future, we will propose a new image segmentation technology with higher accuracy to improve our algorithm.

- Limitation of data: Although our feature selection and prediction algorithms show great performance on the given dataset, we are not sure whether it can work well on larger dataset since the fact that we only have 23 patients. In the future, we will find larger to verify our findings and try to give some more general results which can help doctors to make better diagnose on DR patients and to provide better medical treatment results.

- Model evaluation: In this project, we only use accuracy to evaluate our models. In fact, precision, recall and ROC curves are all widely to measure model's performance in clinical studies. We suggest future studies to adapt more complex evaluation technologies to evaluate the models.

Bibliography

[1] American Diabetes Association et al. Diagnosis and classification of diabetes mellitus. *Diabetes care*, 33(Supplement 1):S62–S69, 2010.

[2] Miguel O Bernabeu, Martin L Jones, Rupert W Nash, Anna Pezzarossa, Peter V Coveney, Holger Gerhardt, and Claudio A Franco. Polnet analysis: a software tool for the quantification of network-level endothelial cell polarity and blood flow during vascular remodelling. *BioRxiv*, 2017.

[3] Miguel O Bernabeu, Martin L Jones, Jens H Nielsen, Timm Krüger, Rupert W Nash, Derek Groen, Sebastian Schmieschek, James Hetherington, Holger Gerhardt, Claudio A Franco, et al. Computer simulations reveal complex distribution of haemodynamic forces in a mouse retina model of angiogenesis. *Journal of the Royal Society Interface*, 11(99):20140543, 2014.

[4] Sumit Bhatia, Bapi Chatterjee, Deepak Nathani, and Manohar Kaul. Understanding and predicting links in graphs: A persistent homology perspective. *arXiv preprint arXiv:1811.04049*, 2018.

[5] Ed Bullmore and Olaf Sporns. Complex brain networks: graph theoretical analysis of structural and functional systems. *Nature reviews neuroscience*, 10(3):186, 2009.

[6] Amram Eshel and Tom Beeckman. *Plant roots: the hidden half*. CRC press, 2013.

[7] Chris Florkowski. Hba1c as a diagnostic test for diabetes mellitus–reviewing the evidence. *The Clinical Biochemist Reviews*, 34(2):75, 2013.

[8] Muhammad Moazam Fraz, Paolo Remagnino, Andreas Hoppe, Bunyarit Uyyanonvara, Alicja R Rudnicka, Christopher G Owen, and Sarah A Barman.

Blood vessel segmentation methodologies in retinal images–a survey. *Computer methods and programs in biomedicine*, 108(1):407–433, 2012.

[9] Florentina J Freiberg, Maximilian Pfau, Juliana Wons, Magdalena A Wirth, Matthias D Becker, and Stephan Michels. Optical coherence tomography angiography of the foveal avascular zone in diabetic retinopathy. *Graefe's Archive for Clinical and Experimental Ophthalmology*, 254(6):1051–1058, 2016.

[10] SJ Griffin, PS Little, CN Hales, AL Kinmonth, and NJ Wareham. Diabetes risk score: towards earlier detection of type 2 diabetes in general practice. *Diabetes/metabolism research and reviews*, 16(3):164–171, 2000.

[11] Luis Gruberg, George Dangas, Roxana Mehran, Gary S Mintz, Kenneth M Kent, Augusto D Pichard, Lowell F Satler, Alexandra J Lansky, Gregg W Stone, and Martin B Leon. Clinical outcome following percutaneous coronary interventions in patients with chronic renal failure. *Catheterization and cardiovascular interventions*, 55(1):66–72, 2002.

[12] Aric Hagberg, Pieter Swart, and Daniel S Chult. Exploring network structure, dynamics, and function using networkx. Technical report, Los Alamos National Lab.(LANL), Los Alamos, NM (United States), 2008.

[13] Robert E Horton. Erosional development of streams and their drainage basins; hydrophysical approach to quantitative morphology. *Geological society of America bulletin*, 56(3):275–370, 1945.

[14] Ioannis Iakovou, George Dangas, Roxana Mehran, Alexandra J Lansky, Dale T Ashby, Martin Fahy, Gary S Mintz, Kenneth M Kent, Augusto D Pichard, Lowell F Satler, et al. Impact of gender on the incidence and outcome of contrast-induced nephropathy after percutaneous coronary intervention. *The Journal of invasive cardiology*, 15(1):18–22, 2003.

[15] Masayuki Iwasaki and H Inomata. Relation between superficial capillaries and foveal structures in the human retina. *Investigative ophthalmology & visual science*, 27(12):1698–1705, 1986.

[16] Ghassan S Kassab. Scaling laws of vascular trees: of form and function. *American Journal of Physiology-Heart and Circulatory Physiology*, 290(2):H894–H903, 2006.

[17] Eleni Katifori and Marcelo O Magnasco. Quantifying loopy network architectures. *PloS one*, 7(6):e37994, 2012.

[18] Alan Kennedy and Joël Pynte. Parafoveal-on-foveal effects in normal reading. *Vision research*, 45(2):153–168, 2005.

[19] Brian D Krawitz, Shelley Mo, Lawrence S Geyman, Steven A Agemy, Nicole K Scripsema, Patricia M Garcia, Toco YP Chui, and Richard B Rosen. Acircularity index and axis ratio of the foveal avascular zone in diabetic eyes and healthy controls measured by optical coherence tomography angiography. *Vision research*, 139:177–186, 2017.

[20] Junki Kwon, Jaewan Choi, Joong Won Shin, Jiyun Lee, and Michael S Kook. Alterations of the foveal avascular zone measured by optical coherence tomography angiography in glaucoma patients with central visual field defects. *Investigative ophthalmology & visual science*, 58(3):1637–1645, 2017.

[21] Hyungwoo Lee, Minsub Lee, Hyewon Chung, and Hyung Chan Kim. Quantification of retinal vessel tortuosity in diabetic retinopathy using optical coherence tomography angiography. *Retina*, 38(5):976–985, 2018.

[22] Jie Lian. Computational approaches to vascular network analysis. 4 2019.

[23] Gerald Liew, Jie Jin Wang, Paul Mitchell, and Tien Y Wong. Retinal vascular imaging: a new tool in microvascular disease research. *Circulation: Cardiovascular Imaging*, 1(2):156–161, 2008.

[24] Jaana Lindström and Jaakko Tuomilehto. The diabetes risk score: a practical tool to predict type 2 diabetes risk. *Diabetes care*, 26(3):725–731, 2003.

[25] Huan Liu and Hiroshi Motoda. *Computational methods of feature selection*. CRC Press, 2007.

[26] TJ MacGillivray, Emanuele Trucco, JR Cameron, Baljean Dhillon, JG Houston, and EJR Van Beek. Retinal imaging as a source of biomarkers for diagnosis, characterization and prognosis of chronic illness or long-term conditions. *The British journal of radiology*, 87(1040):20130832, 2014.

[27] Ian Mauldin. Analyzing the local spatial structure of vascular networks. Master's thesis, University of Edinburgh, 7 2018.

[28] Yuriy Mileyko, Herbert Edelsbrunner, Charles A Price, and Joshua S Weitz. Hierarchical ordering of reticular networks. *PLoS One*, 7(6):e36715, 2012.

[29] Bojan Mohar. Some applications of laplace eigenvalues of graphs. In *Graph symmetry*, pages 225–275. Springer, 1997.

[30] K Narasimhan, VC Neha, and K Vijayarekha. An efficient automated system for detection of diabetic retinopathy from fundus images using support vector machine and bayesian classifiers. In *2012 International Conference on Computing, Electronics and Electrical Technologies (ICCEET)*, pages 964–969. IEEE, 2012.

[31] WI Newman, DL Turcotte, and AM Gabrielov. Fractal trees with side branching. *Fractals*, 5(04):603–614, 1997.

[32] Johannes Reichold, Marco Stampanoni, Anna Lena Keller, Alfred Buck, Patrick Jenny, and Bruno Weber. Vascular graph model to simulate the cerebral blood flow in realistic vascular networks. *Journal of Cerebral Blood Flow & Metabolism*, 29(8):1429–1443, 2009.

[33] Hideki Shiihara, Hiroto Terasaki, Shozo Sonoda, Naoko Kakiuchi, Yuki Shinohara, Masatoshi Tomita, and Taiji Sakamoto. Objective evaluation of size and shape of superficial foveal avascular zone in normal subjects by optical coherence tomography angiography. *Scientific reports*, 8(1):10143, 2018.

[34] Arthur N Strahler. Quantitative analysis of watershed geomorphology. *Eos, Transactions American Geophysical Union*, 38(6):913–920, 1957.

[35] Rowan Sugden. Analyzing the local spatial structure of vascular networks. Master's thesis, University of Edinburgh, 7 2018.

[36] William V Tamborlane, Raymond L Hintz, Michael Bergman, Myron Genel, Philip Felig, and Robert S Sherwin. Insulin-infusion-pump treatment of diabetes: influence of improved metabolic control on plasma somatomedin levels. *New England Journal of Medicine*, 305(6):303–307, 1981.

[37] DL Turcotte, JD Pelletier, and WI Newman. Networks with side branching in biology. *Journal of Theoretical Biology*, 193(4):577–592, 1998.

[38] Aki Vehtari, Andrew Gelman, and Jonah Gabry. Practical bayesian model evaluation using leave-one-out cross-validation and waic. *Statistics and computing*, 27(5):1413–1432, 2017.

Appendix A

Feature changes Plots

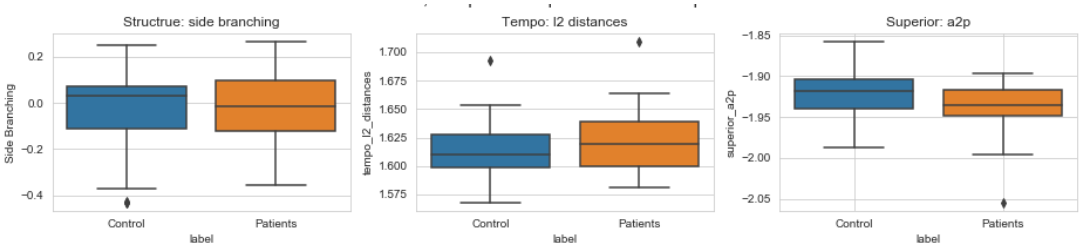

Figure A.1: Classification Other Boxplots

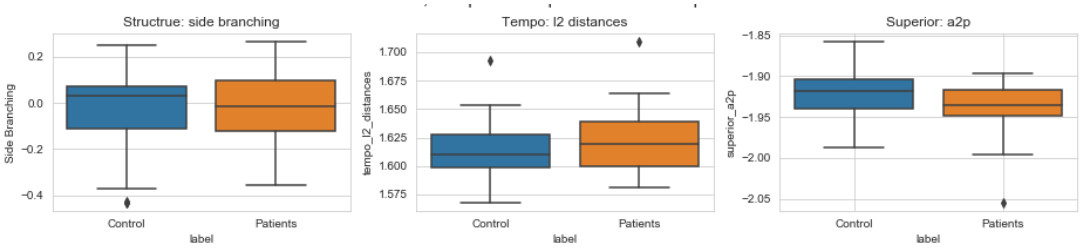

Figure A.2: Classification Other Boxplots

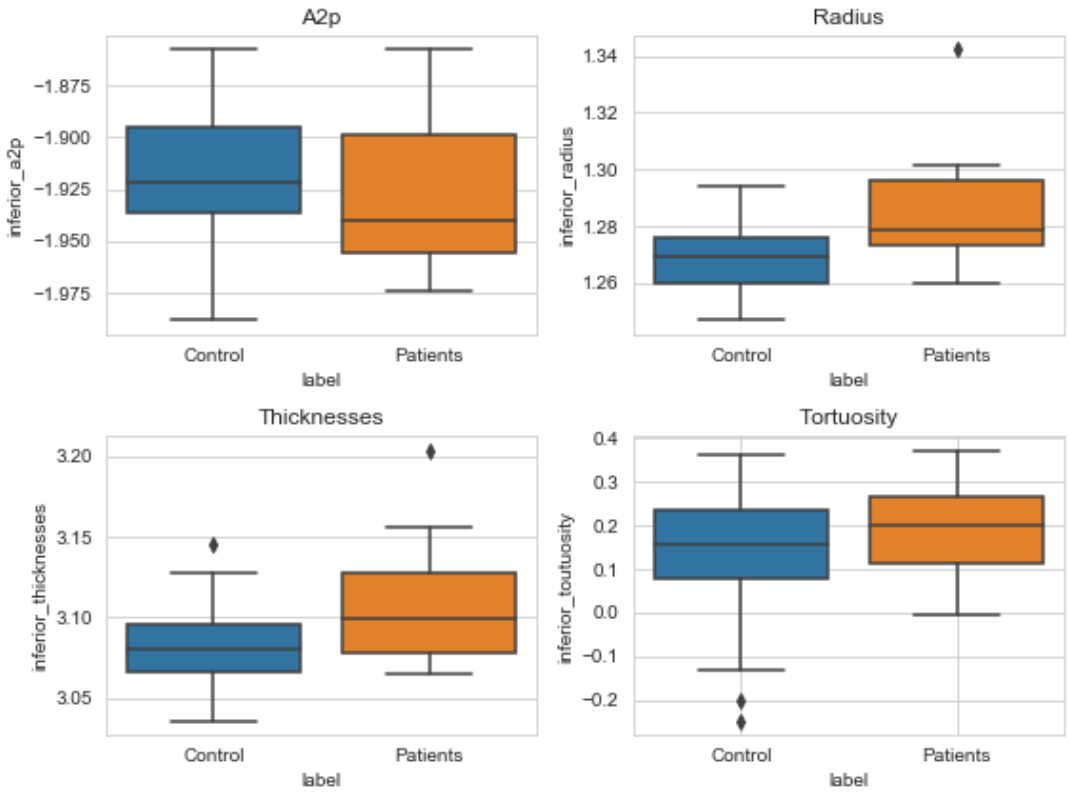

Figure A.3: Classification Inferior Boxplots

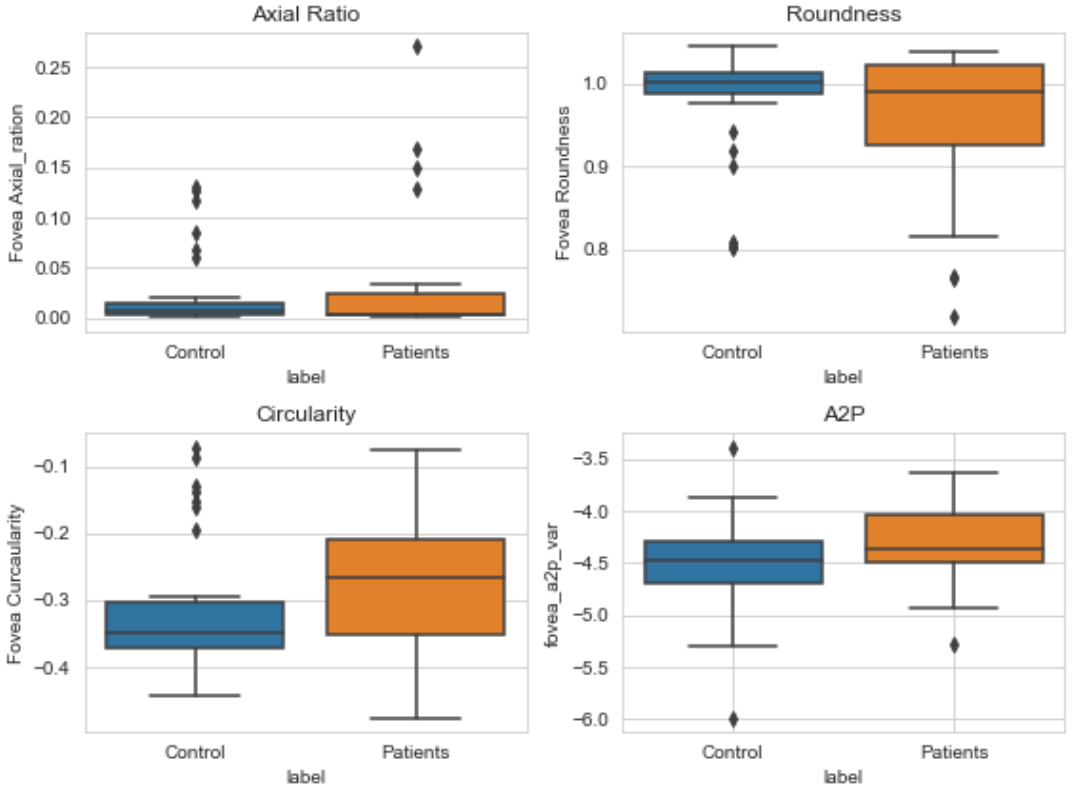

Figure A.4: Classification fovea Boxplots

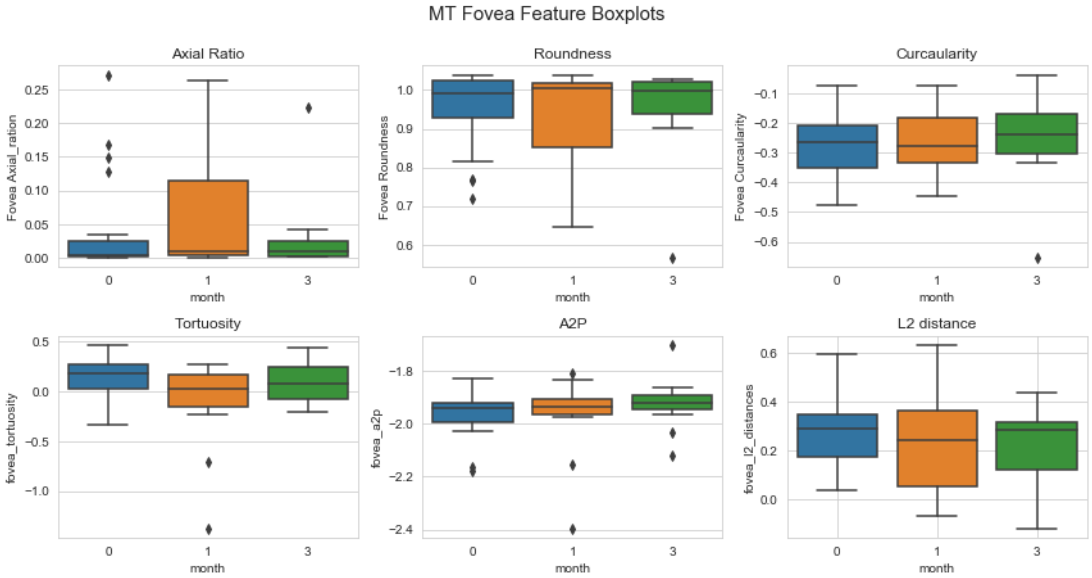

Figure A.5: Prediction Fovea Boxplots